Contribution from the ISSECC, CNR, and Department of Chemistry, University of Florence, Florence, Italy

Anisotropic Exchange in Transition-Metal Dinuclear Complexes. 6.[1] Bis(μ-chloro)bis(dichlorocuprates(II))

A. BENCINI,[2a] D. GATTESCHI,*[2b] and C. ZANCHINI[2b]

Received May 8, 1984

Single-crystal EPR spectra of $[(C_6H_5)_4A]_2Cu_2Cl_6$, A = P, Sb, have been recorded at two different frequencies in a range of temperatures. The zero-field splitting tensors were found to have the largest component perpendicular to the Cu–Cu direction, thus showing the presence of a substantial exchange contribution to the anisotropic spin–spin interaction, as was previously observed for the arsonium derivative. In order to have structural parameters available for all the complexes, the X-ray crystal structure of $[(C_6H_5)_4Sb]_2Cu_2Cl_6$ was determined at room temperature. The crystals are isomorphous with the phosphonium and arsonium derivatives, belonging to the monoclinic space group $P2_1/n$, with a = 13.412 (4) Å, b = 19.894 (4) Å, c = 9.501 (2) Å, β = 109.6 (3)°, and Z = 2. Least-squares refinement of the structure led to a conventional R factor of 0.025. A reanalysis of the magnetic susceptibility data of the arsonium complex showed that the exchange coupling constant does not vary significantly in the series. The zero-field splitting tensor however does vary, the largest value being observed for the phosphonium and the smallest for the stibonium derivative. This behavior has been related to the increased metal–metal distance observed on passing from the phosphonium to the stibonium through arsonium derivatives in agreement with a general trend observed also for the bis(μ-oxo)-bridged copper(II) complexes.

Introduction

Two interacting copper(II) ions yield a singlet and a triplet state, whose energy separation is given by the isotropic exchange coupling constant. The triplet is generally split even in the absence of an external magnetic field. The splitting is best determined through EPR measurements, which yield the so-called zero-field splitting tensor **D**. The principal values and directions of this tensor are determined by the electronic structure of the dinuclear unit, since they depend on the metal–metal distance, on the geometry of the bridge connecting the two metal ions, and on the relative orientation of the molecular axes of the two copper ions. It is apparent therefore that structural information is contained in the zero-field splitting tensor, but as yet not many efforts have been made to study series of analogous complexes in order to relate the experimentally determined **D** tensor to the electronic structure of the interacting pairs.[3]

We have recently reported that in bis(μ-oxo)-bridged copper(II) complexes in which the bridging ligands occupy equatorial positions of tetragonal coordination polyhedra the largest zero-field splitting component is found orthogonal to the equatorial planes and to the copper–copper direction, thus showing that **D** is mainly determined by exchange contributions.[1,4-6] We also showed that the often assumed $(\Delta g/g)^2J$ dependence of **D** does not hold.[7]

In order to extend the study to other similar series of complexes, we took into consideration the chlorocuprates $[(C_6H_5)_4A]_2Cu_2Cl_6$ (A = P, As, Sb). For the phosphonium, *p*, and the arsonium, *as*, derivatives the crystal structures were previously determined,[8,9] showing that the two copper ions are bridged by two chlorine atoms, the coordination environment around each copper ion being a distorted tetrahedron. For the three complexes the temperature dependence of the magnetic susceptibility has been used to obtain the isotropic exchange coupling constant, which is ferromagnetic in the whole series.[10,11] Polycrystalline powder EPR spectra have been reported for the three complexes[11,12] showing that the zero-field splitting parameter D is on the order of 0.11 cm^{-1}. Single-crystal EPR spectra of *as* showed that the largest zero-field splitting component is found orthogonal to the copper–copper direction.[12]

We have now determined the X-ray crystal structure of the stibonium complex and have recorded the single-crystal EPR spectra of the phosphonium and stibonium derivatives in order to discuss the variation of the isotropic exchange coupling constant and of the zero-field splitting tensors having the full set of structural, magnetic, and EPR data available for the whole series.

Table I. Summary of Crystal Data and Intensity Data Collection

formula	$C_{48}H_{40}Cl_6Cu_2Sb_2$
cryst syst, space group	monoclinic, $P2_1/n$
a, Å	13.412 (4)
b, Å	19.894 (4)
c, Å	9.501 (2)
β, deg	109.6 (3)
V, Å^3	2388.9
Z	2
D_{calcd}, g cm^{-3}	1.668
μ(Mo Kα), cm^{-1}	22.28
transmission factors, max-min	0.84-0.55
scan type	ω-2θ
scan speed, deg min^{-1}	3
scan width ($\Delta\omega$), deg	0.8 + 0.30 tan θ
bkgd	stationary counter-stationary cryst symmetric, at each end of scan
collection range	$\pm h,k,l$ ($2\theta < 44°$)
no. of data	2579
no. of data, $I > 3\sigma(I)$	2221
no. of variables	262
R^a	0.025
$R_w{}^a$	0.025

^{a} $R = \Sigma||F_o|-|F_c||/\Sigma|F_o|$; $R_w = [\Sigma w(|F_o|-|F_c|)^2/\Sigma w(F_o)^2]^{1/2}$.

Experimental Section

The chlorocuprates $[(C_6H_5)_4A]_2Cu_2Cl_6$ (A = P, As, Sb) were prepared as previously described.[11] Single crystals were grown by slow evaporation of ethanol solutions of the complexes.

EPR spectra were recorded with a Varian E9 spectrometer, equipped with both X- and Q-band frequencies. Variable-temperature spectra were recorded with use of standard Varian apparatus down to liquid-nitrogen temperature and with an Oxford Instruments ESR9 continuous-flow cryostat below that limit. Single-crystal spectra were obtained by mounting the crystals on a Perspex rod. At X-band the rod was rotated with a one-circle goniometer, while at Q-band the magnet was rotated.

(1) Part 5: Bencini, A.; Gatteschi, D.; Zanchini, C. *Inorg. Chem.*, preceding paper in this issue.
(2) (a) ISSECC, CNR. (b) University of Florence.
(3) Smith, T. D.; Pilbrow, J. R. *Coord. Chem. Rev.* **1974**, *13*, 173.
(4) Banci, L.; Bencini, A.; Gatteschi, D. *J. Am. Chem. Soc.* **1983**, *105*, 761.
(5) Banci, L.; Bencini, A.; Gatteschi, D.; Zanchini, C. *J. Magn. Reson.* **1982**, *48*, 9.
(6) Bencini, A.; Gatteschi, D. In "Structural-Magnetic Correlations in Exchange Coupled Systems"; Willett, R. D., Gatteschi, D., Kahn, O., Eds.; D. Reidel: Dordrecht, The Netherlands, 1985; p 241.
(7) Bencini, A.; Di Vaira, M.; Fabretti, A. C.; Gatteschi, D.; Zanchini, C. *Inorg. Chem.* **1984**, *23*, 1620.
(8) Willett, R. D.; Chow, C. *Acta Crystallogr., Sect. B: Struct. Crystallogr. Cryst. Chem.* **1974**, *B30*, 207.
(9) Textor, M.; Dubler, E.; Oswald, H. R. *Inorg. Chem.* **1974**, *13*, 1361.
(10) Chow, C.; Caputo, R.; Willett, R. D.; Gerstein, B. C. *J. Chem. Phys.* **1974**, *61*, 271.
(11) Estes, W. E.; Wasson, J. R.; Hall, J. W.; Hatfield, W. E. *Inorg. Chem.* **1978**, *17*, 3657.
(12) Chow, C.; Willett, R. D. *J. Chem. Phys.* **1973**, *59*, 5903.

0020-1669/85/1324-0704$01.50/0

Table II. Positional Parameters for the Non-hydrogen Atoms for $[(C_6H_5)_4Sb]_2Cu_2Cl_6$[a]

atom	x	y	z
Sb	5345	2934	8543
Cu	1068 (1)	4586	−144 (1)
Cl1	−603 (1)	4912 (1)	−1714 (1)
Cl2	2780 (1)	4811 (1)	792 (2)
Cl3	1137 (1)	3660 (1)	−1353 (2)
C11	6700 (4)	2786 (3)	7949 (5)
C12	6934 (4)	2145 (3)	7582 (6)
C13	7853 (5)	2034 (3)	7267 (7)
C14	8530 (5)	2550 (4)	7341 (7)
C15	8295 (4)	3194 (3)	7675 (6)
C16	7381 (4)	3317 (3)	7987 (5)
C21	4294 (4)	3588 (3)	7030 (5)
C22	4571 (5)	3864 (3)	5867 (6)
C23	3857 (6)	4272 (4)	4830 (7)
C24	2883 (6)	4387 (3)	4934 (8)
C25	2603 (5)	4115 (3)	6078 (8)
C26	3318 (4)	3711 (3)	7142 (7)
C31	4605 (4)	1991 (3)	8392 (6)
C32	4036 (4)	1764 (3)	6974 (6)
C33	3580 (4)	1134 (3)	6818 (7)
C34	3688 (5)	741 (3)	8041 (8)
C35	4265 (4)	972 (3)	9453 (7)
C36	4730 (4)	1604 (3)	9651 (6)
C41	5741 (4)	3327 (3)	10708 (5)
C42	6339 (4)	2947 (3)	11916 (6)
C43	6611 (5)	3211 (4)	13349 (6)
C44	6296 (5)	3852 (4)	13541 (7)
C45	5695 (5)	4226 (3)	12343 (7)
C46	5407 (4)	3965 (3)	10916 (6)

[a] Coordinates multiplied by 10^4.

Diffuse-reflectance spectra were recorded on a Beckman DK2 spectrophotometer, equipped with a homemade cryostat. Liquid nitrogen and dry ice–acetone were used for varying the temperature.

Single crystals of $[(C_6H_5)_4P]_2Cu_2Cl_6$ were found to correspond to the reported structure,[9] space group $P2_1/c$, with $a = 9.226$ Å, $b = 19.301$ Å, $c = 13.848$ Å, and $\beta = 111.26°$.

X-ray Structure Determination. A crystal of the compound $[(C_6H_5)_4Sb]_2Cu_2Cl_6$ shaped as a rhombic prism with dimensions 0.10 × 0.32 × 0.35 mm was used for crystal data and intensity data collection. A Philips PW 1100 automated diffractometer with graphite-monochromated Mo Kα radiation was used for all the operations. Lattice constants were determined at 20 °C from the setting angles of 22 reflections with $8° < \theta < 14°$. Details of crystal data and data collection are listed in Table I. No systematic variation of intensity of three standard reflections measured every 120 min was observed. The data were corrected for Lorentz and polarization effects as well as for absorption. The principal computer programs used in the crystallographic calculations are listed in ref 13. The positions of the stibonium and copper atoms were determined with use of direct methods, and those of all the other non-hydrogen atoms were found in subsequent Fourier maps. The structure was refined with use of a full-matrix least-squares method based on minimization of the function $\sum w(|F_o| - |F_c|)^2$ with weights $w = 1/\sigma^2(F_o)$. Anisotropic thermal parameters were used for all the non-hydrogen atoms. Hydrogen atoms were introduced in calculated positions (C–H = 1.08 Å) as fixed contributions, each with a temperature factor 20% larger than that of the isotropic equivalent of the respective carbon atom. The scattering factors for the neutral atoms were taken from ref 14 and the anomalous correction terms from ref 15. The final R values were $R = 0.025$, $R_w = 0.025$. The highest peaks in the final difference map were less than 0.5 e Å^{-3}. The final positional parameters for the non-hydrogen atoms are given in Table II. Listings of the thermal parameters for the non-hydrogen atoms and of hydrogen atom coordinates (Tables SI and SII) and of observed and calculated structure

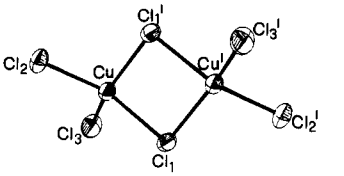

Figure 1. The $[Cu_2Cl_6]^{2-}$ ion in $[(C_6H_5)_4Sb]_2Cu_2Cl_6$. The view is perpendicular to the Cu–Cl(1)–Cu′ plane.

Table III. Interatomic Distances (Å) of $[(C_6H_5)_4Sb]_2Cu_2Cl_6$

(I) Distances within the $[Cu_2Cl_6]^{2-}$ Ion			
Cu–Cl(1)	2.336 (2)	Cu–Cl(1′)	2.290 (2)
Cu–Cl(2)	2.212 (1)	Cu–Cu′	3.400 (3)
Cu–Cl(3)	2.189 (2)		
(II) Distances within the $[(C_6H_5)_4Sb]^+$ Ion			
Sb–C(11)	2.098 (5)	Sb–C(31)	2.104 (5)
Sb–C(21)	2.094 (5)	Sb–C(41)	2.095 (5)
C(11)–C(12)	1.385 (7)	C(31)–C(32)	1.382 (7)
C(12)–C(13)	1.380 (7)	C(32)–C(33)	1.382 (7)
C(13)–C(14)	1.356 (8)	C(33)–C(34)	1.367 (7)
C(14)–C(15)	1.382 (8)	C(34)–C(35)	1.383 (8)
C(15)–C(16)	1.377 (7)	C(35)–C(36)	1.388 (7)
C(16)–C(11)	1.390 (6)	C(36)–C(31)	1.385 (7)
C(21)–C(22)	1.392 (7)	C(41)–C(42)	1.384 (7)
C(22)–C(23)	1.383 (8)	C(42)–C(43)	1.389 (7)
C(23)–C(24)	1.363 (8)	C(43)–C(44)	1.374 (8)
C(24)–C(25)	1.373 (9)	C(44)–C(45)	1.373 (8)
C(25)–C(26)	1.393 (8)	C(45)–C(46)	1.381 (7)
C(26)–C(21)	1.370 (7)	C(46)–C(41)	1.382 (7)

[a] Estimated standard deviations in parentheses.

Table IV. Interatomic Angles (deg)[a] of $[(C_6H_5)_4Sb]_2Cu_2Cl_6$

(I) Angles within the $[Cu_2Cl_6]^{2-}$ Ion			
Cl(1)–Cu–Cl(2)	147.9 (1)	Cl(2)–Cu–Cl(3)	99.2 (1)
Cl(1)–Cu–Cl(3)	95.7 (1)	Cl(1′)–Cu–Cl(2)	96.7 (1)
Cl(3)–Cu–Cl(1′)	147.4 (1)	Cl(1)–Cu–Cl(1′)	85.4 (1)
Cu–Cl(1)–Cu′	94.6 (1)		
(II) Angles within the $[(C_6H_5)_4Sb]^+$ Ion			
C(11)–Sb–C(21)	110.3 (2)	C(21)–Sb–C(31)	108.2 (2)
C(11)–Sb–C(31)	106.7 (2)	C(21)–Sb–C(41)	109.5 (2)
C(11)–Sb–C(41)	111.0 (2)	C(31)–Sb–C(41)	111.0 (2)
C(11)–C(12)–C(13)	119.8 (5)	C(31)–C(32)–C(33)	118.8 (5)
C(12)–C(13)–C(14)	119.9 (6)	C(32)–C(33)–C(34)	120.7 (5)
C(13)–C(14)–C(15)	120.9 (5)	C(33)–C(34)–C(35)	120.0 (5)
C(14)–C(15)–C(16)	120.1 (5)	C(34)–C(35)–C(36)	120.8 (5)
C(15)–C(16)–C(11)	119.0 (5)	C(35)–C(36)–C(31)	117.9 (5)
C(16)–C(11)–C(12)	120.2 (5)	C(36)–C(31)–C(32)	121.8 (5)
C(21)–C(22)–C(23)	119.5 (6)	C(41)–C(42)–C(43)	119.7 (5)
C(22)–C(23)–C(24)	119.9 (6)	C(42)–C(43)–C(44)	119.3 (6)
C(23)–C(24)–C(25)	120.9 (6)	C(43)–C(44)–C(45)	120.9 (6)
C(24)–C(25)–C(26)	119.9 (6)	C(44)–C(45)–C(46)	120.2 (6)
C(25)–C(26)–C(21)	119.3 (6)	C(45)–C(46)–C(41)	119.2 (5)
C(26)–C(21)–C(22)	120.5 (5)	C(46)–C(41)–C(42)	120.6 (5)

[a] Estimated standard deviations in parentheses.

Table V. Structural Parameters Relevant to the Exchange Interaction in $[(C_6H_5)A]_2Cu_2Cl_6$ (A = P, As, Sb)

	P	as	sb
Cu–Cu, Å	3.355 (1)	3.382 (1)	3.400 (3)
$Cu–Cl_1$,[a] Å	2.321 (2)	2.333 (2)	2.336 (2)
$Cu–Cl_2$,[a] Å	2.292 (2)	2.305 (2)	2.290 (2)
ϕ,[b] deg	93.3 (1)	93.7 (1)	94.6 (1)
α,[b] deg	50	48.2	44.4
β_1,[b] deg	143.6 (1)	145.2 (1)	147.9 (1)
β_2,[b] deg	143.3 (1)	144.6 (1)	147.4 (1)

[a] Bridging chlorines. [b] See text.

(13) (a) Stewart, J. M.; Kundall, F. A.; Baldwin, J. C. "X-Ray 72 System of Programs", Technical Report TR 1982; University of Maryland: College Park, MD, 1972. (b) Sheldrick, G. "SHELX 76 System of Computing Programs"; University of Cambridge: Cambridge, England, 1976. (c) Johnson, C. K. *Oak Ridge Natl. Lab., [Rep.] ORNL (U.S)* **1965**, *ORNL-3794*.

(14) "International Tables for X-ray Crystallography"; Kynoch Press: Birmingham, England, 1974; Vol. IV, p 71 ff.

(15) Corfield, P. W. R.; Doedens, R. J.; Ibers, J. A. *Inorg. Chem.* **1967**, *6*, 197.

(16) See paragraph at the end of the paper regarding supplementary material.

(17) Hay, J. P.; Thibeault, J. C.; Hoffmann, R. *J. Am. Chem. Soc.* **1975**, *97*, 4884.

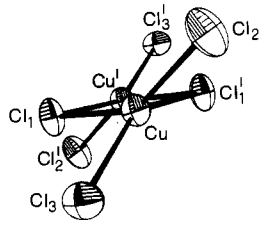

Figure 2. The $[Cu_2Cl_6]^{2-}$ ion in $[(C_6H_5)_4Sb]_2Cu_2Cl_6$ viewed approximately along the copper–copper direction.

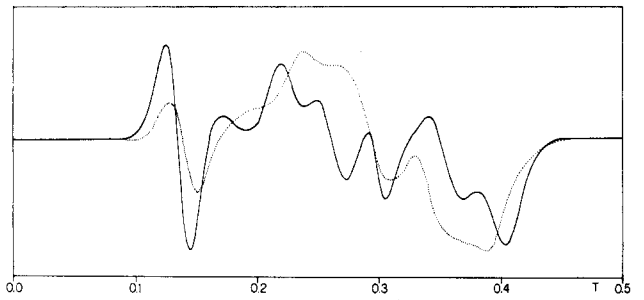

Figure 3. Polycrystalline powder EPR spectra of $[(C_6H_5)_4Sb]_2Cu_2Cl_6$: (···) room temperature; (—) 4.2 K.

amplitudes are available as supplementary material.

Results

Description of the Structure of *sb*. The crystal structure of *sb* is essentially identical with that of the *p* and *as* homologues,[8,9] containing isolated $Cu_2Cl_6^{2-}$ units, shown in Figure 1. Intramolecular distances and angles are given in Tables III and IV, respectively. The copper–copper distance of 3.400 (3) Å is the largest observed in the series, as shown in Table V, where a comparison of the structural parameters of *p*, *as*, and *sb* that are relevant to the exchange interaction are given. The $Cu_2Cl_6^{2-}$ units are nonplanar, with the dihedral angle α, formed by the planes defined by the copper atom and the terminal chlorines and the copper atom and the bridging chlorines, respectively, of 44.4°, as shown in Figure 2. In *p* α is 50° and in *as* 48°: therefore, the *sb* derivative is that showing the minimum deviation from the planar coordination in the series. The same conclusions can be reached by looking at the largest angles in the coordination polyhedron of each copper ion, β_1 and β_2 (see Table V). These angles are approximately bisected by the compression axis of the tetrahedra; they would be 180° for a square-planar and 90° for a tetrahedral chromophore. The largest value observed for *sb* shows that this is closest to the square-planar limit.

The distances to the terminal chlorines in *sb* (2.211 (1) and 2.189 (2) Å) are different from each other, as observed also for the other derivatives, and slightly longer than those of *p* and *as*. According to McGinnety[18] the electrostatic forces in the lattice shorten the Cu–Cl bonds in Cs_2CuCl_4. If the same model is applied to the *p*, *as*, and *sb* derivatives, the longer bonds observed for *sb* might be due to the larger dimensions of the cation. To this same effect might be ascribed also the smaller tetrahedral distortion observed in *sb*. Less regular variations are observed in the bridging-chlorine distances throughout the series.

The tetraphenylstibonium cation has the expected tetrahedral configuration around Sb, the average C–Sb–C angle corresponding nicely to the average seen in *p*[9] and *as*[8] (109.45° for *sb*, 109.45° for *p*, and 109.47° for *as*). The Sb–C distances are distinctly longer than the P–C and As–C distances (2.098 Å for *sb*, 1.906 Å for *as*, and 1.775 Å for *p*).

EPR Spectra. Polycrystalline powder EPR spectra of *sb* at room temperature and at 4.2 K are shown in Figure 3. They are typical of a triplet state as expected for the $Cu_2Cl_6^{2-}$ species and are temperature dependent, the zero-field splitting increasing on lowering the temperature. Single-crystal spectra were recorded

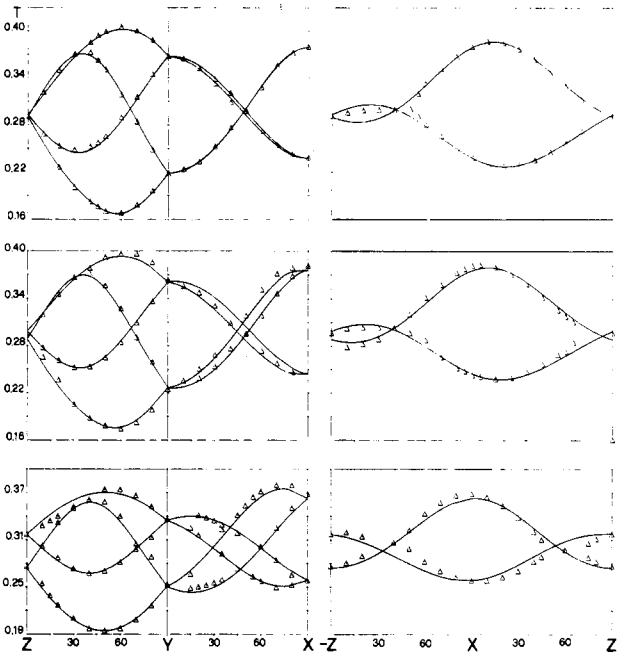

Figure 4. Angular dependence of the transition fields at X-band frequency for $[(C_6H_5)_4Sb]_2Cu_2Cl_6$: (upper) 4.2 K; (middle) 140 K; (lower) room temperature.

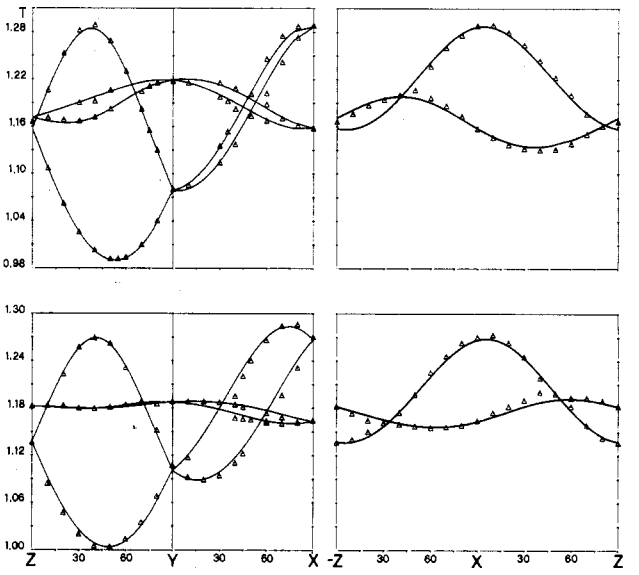

Figure 5. Angular dependence of the transition fields at Q-band frequency for $[(C_6H_5)_4Sb]_2Cu_2Cl_6$: (upper) 140 K; (lower) room temperature.

at room temperature and 140 and 4.2 K. At the last temperature only X-band spectra were recorded, while at 140 K and room temperature both X- and Q-band frequencies were employed. The resonant fields were found to be temperature dependent, in agreement with the polycrystalline powder spectra, but the number of magnetically nonequivalent sites does not change, and the symmetry relations between them remain unaltered. Therefore, we have no evidence of a phase transition, but as far as the EPR spectra can be diagnostic, the unit cell remains monoclinic in the entire investigated temperature range.

The angular dependences of the transition fields of *sb* in three orthogonal crystal planes at X- and Q-band frequencies are shown in Figures 4 and 5, respectively. The curves were calculated through a previously described least-squares fitting procedure that allows for nonparallel **g** and **D** tensor axes.[5]

The **g** and **D** tensors at room temperature and 140 and 4.2K are given in Table VI. The **g** tensor is quasi-axial, the highest *g* value, 2.308 (3) at room temperature, 2.295 (2) at 140 K, and

(18) McGinnety, J. A. *J. Am. Chem. Soc.* **1972**, *94*, 8406.

Table VI. Principal Values and Directions of the **g** and **D** Tensors at Room Temperature, 140 K, and 4.2 K for $[(C_6H_5)_4Sb]_2Cu_2Cl_6$[a]

g_{xx}	g_{yy}	g_{zz}	$D_{x'x'}$[b]	$D_{y'y'}$[b]	$D_{z'z'}$[b]
		Room Temperature			
2.044 (3)	2.063 (2)	2.308 (2)	0.0468 (8)	0.0174 (7)	−0.0642 (6)
0.55 (7)	0.82 (5)	0.183 (8)	0.78 (1)	0.61 (1)	0.127 (6)
0.62 (2)	−0.25 (5)	−0.739 (3)	0.41 (1)	−0.439 (8)	−0.766 (2)
0.56 (4)	−0.52 (5)	0.648 (4)	0.469 (8)	−0.657 (8)	0.630 (3)
		140 K			
2.035 (2)	2.070 (2)	2.295 (2)	0.0314 (7)	0.0476 (8)	−0.0791 (6)
0.60 (3)	0.79 (2)	−0.040 (9)	0.56 (2)	0.82 (1)	0.104 (5)
0.51 (2)	−0.42 (2)	−0.747 (3)	0.513 (7)	−0.25 (1)	−0.821 (2)
0.61 (2)	−0.42 (2)	0.663 (3)	0.61 (2)	−0.52 (1)	0.561 (2)
		4.2 K			
2.047 (5)	2.058 (5)	2.285 (4)	0.0269 (5)	0.0576 (6)	−0.0845 (4)
0.6 (1)	0.8 (1)	−0.07 (1)	0.637 (8)	0.766 (6)	0.080 (3)
0.5 (1)	−0.5 (1)	−0.747 (7)	0.465 (4)	−0.299 (5)	−0.833 (1)
0.6 (1)	−0.4 (1)	0.661 (8)	0.614 (6)	−0.568 (6)	0.547 (1)

[a] The directions are given as cosines referred to *X*, *Y*, *Z* axes, with *Y* parallel to *b* and *X* parallel to the $\bar{1}01$ face. [b] In cm^{-1}.

Table VII. Principal Values and Directions of the **g** and **D** Tensors at Room Temperature for $[(C_6H_5)_4P]_2Cu_2Cl_6$ for the Two Magnetically Nonequivalent Sites[a]

g_{xx}	g_{yy}	g_{zz}	$D_{x'x'}$[b]	$D_{y'y'}$[b]	$D_{z'z'}$[b]
		Site I			
2.037 (9)	2.063 (8)	2.332 (9)	0.017 (1)	0.056 (1)	−0.073 (1)
−0.3 (1)	−0.35 (9)	−0.90 (1)	−0.426 (9)	−0.11 (1)	−0.897 (4)
0.2 (2)	−0.93 (7)	0.30 (2)	−0.43 (1)	−0.848 (7)	0.310 (6)
−0.94 (3)	−0.1 (3)	0.32 (2)	−0.797 (9)	0.52 (1)	0.313 (8)
		Site II			
2.02 (1)	2.06 (1)	2.316 (8)	0.014 (1)	0.059 (1)	−0.0740 (9)
0.4 (1)	0.85 (7)	0.36 (2)	0.60 (1)	0.712 (9)	0.361 (6)
−0.44 (3)	−0.17 (8)	0.88 (1)	0.034 (9)	−0.474 (4)	0.879 (2)
0.81 (8)	−0.5 (1)	0.31 (2)	−0.797 (9)	0.52 (1)	0.310 (7)

[a] The directions are given as cosines referred to the *X*, *Y*, *Z* axes with *Z* parallel to *c* and *X* orthogonal to the $1\bar{1}0$ face. [b] In cm^{-1}.

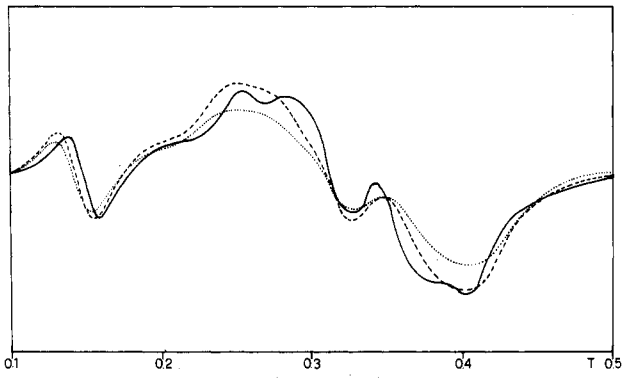

Figure 6. Polycrystalline powder EPR spectra at X-band frequency of (···) $[(C_6H_5)_4P]_2Cu_2Cl_6$, (- - -) $[(C_6H_5)_4As]_2Cu_2Cl_6$, and (—) $[(C_6H_5)_4Sb]_2Cu_2Cl_6$ at room temperature.

2.285 (4) at 4.2 K, being found roughly perpendicular to the mean plane of the six chlorine atoms. The largest zero-field splitting component is also observed parallel to this direction, the angle between g_{zz} and $D_{z'z'}$ being 4 (3)° at room temperature, 11 (1)° at 140 K, and 12 (1)° at 4.2 K. When the temperature is lowered, $D_{z'z'}$ increases in accord with the observations on the polycrystalline powder spectra.

The orientation of the other components of **g**, g_{xx} and g_{yy}, is affected by an error larger than that relative to g_{zz}, since the former values are rather similar to each other. The $D_{x'x'}$ and $D_{y'y'}$ components also show a large variation with temperature, $D_{x'x'}$ decreasing on decreasing temperature and $D_{y'y'}$ increasing. At the same time a rotation of the principal directions occurs, so that the x' axis at 140 K makes an angle of 19 (5)° with the x' axis at room temperature. The y' axis is within error parallel to the Cu–Cu direction at room temperature.

In Figure 6 are shown the polycrystalline powder EPR spectra of *p*, *as*, and *sb* at room temperature. The overall appearance of the spectra is similar for the three complexes, but some significant differences are apparent. In particular a low-field shift of the half-field transition is observed on passing from *sb* to *as* and *p*. This is indicative of an increase of the zero-field splitting in the order *sb*, *as*, *p*. Polycrystalline powder spectra of the three complexes at 4.2 K show the same trend.

The **D** tensor was previously measured for *as*,[12] showing that $D_{z'z'}$ is larger than the value we find for *sb*.

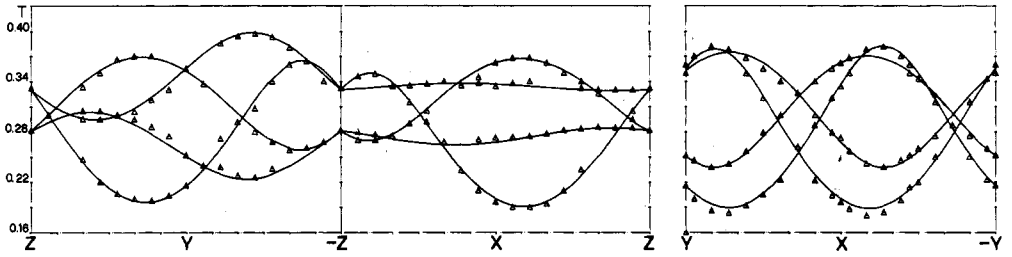

Figure 7. Angular dependence of the transition fields at X-band frequency at room temperature for $[(C_6H_5)_4P]_2Cu_2Cl_6$.

The angular dependence of the transition fields of *p* at room temperature in three mutually orthogonal crystal planes is shown in Figure 7. The **g** and **D** tensors, obtained with the same procedure outlined above for *sb*, are given in Table VII. The fit was independently repeated for the two nonequivalent sites seen in the monoclinic cell. The principal values in the two cases were found to correspond nicely to each other, and the principal directions are related by the symmetry operations of the unit cell. The g_{zz} and $D_{z'z'}$ axes are parallel to each other, within error, and orthogonal to the mean plane of the six chlorine atoms. $D_{y'y'}$ makes an angle of 8° with the Cu–Cu direction, while g_{yy} makes an angle of 40° with it.

Electronic Spectra. Diffuse-reflectance spectra of *sb* were recorded at 77 K, 210 K, and room temperature. The compound shows a broad absorption in the near-IR region, with maxima that shift to higher frequencies as the temperature is lowered. Lowering the temperature causes a neat sharpening of the bands. At room temperature a broad maximum is observed at 11 100 cm^{-1} and at 210 K a peak at 12 600 and a shoulder at ca. 10 000 cm^{-1} is seen, while at 77 K two peaks at 13 100 and 10 100 cm^{-1} are neatly resolved. A similar behavior is observed also for *p* and *as*. The energy of the first charge-transfer band is close to 22 000 cm^{-1} for the three complexes.

Discussion

The structural–magnetic correlations for chloride-bridged copper(II) dimers are still a matter of controversy.[19,20] The present series of *p*, *as*, and *sb* appears to be particularly well suited for finding out a relation between the *J* values and the structural features of the complexes. In fact *J* has been reported to be −80 (9) cm^{-1} for *p*,[11] −46 cm^{-1} for *as*,[10] and −90 (14) cm^{-1} for *sb*.[11] (We are using the spin Hamiltonian in the form $\hat{H} = J\hat{S}_1\cdot\hat{S}_2$). From the reported errors it is apparent that no significant difference is operative between *p* and *sb*. The large errors are due to the intrinsic difficulty in measuring the singlet–triplet splitting of ferromagnetically coupled copper(II) dimers.[21,22] On the other hand, the value for *as*, although no error limit is indicated, appears to be substantially smaller.[10] This is surprising since all the structural parameters of *as* are intermediate between those of *p* and *sb*. In order to estimate the magnitude of the error affecting the *J* value of *as*, we tried to fit again the magnetic susceptibility data, which were reported[10] with use of a least-squares procedure. We found that the calculated error is large, as expected for ferromagnetically coupled copper(II) dimers;[10,21,22] therefore, we conclude that there is not proof that *J* for *as* is significantly different from that of *sb* and *p* and that the extent of the coupling in the three complexes can be substantially unaffected by the variation of the structural parameters. Therefore, plotting *J* vs. the Cu–Cl–Cu angle, ϕ, the Cu–Cu distance, *r*, or the dihedral angle α yields in any case a rather flat curve. The only trend which emerges is that, for a given ϕ angle, the coupling is more intensely ferromagnetic when the coordination is more tetrahedrally distorted. In fact, the value of *J* for chloro[hydrotris(1-pyrazolyl)borato]copper(II),[19] for which $\alpha = 0°$, is −34 cm^{-1}, while for the present compounds, where α is in the range 45–50°, *J* ranges from −80 to −90 cm^{-1}.

The EPR spectra of the three complexes at room temperature indicate that the exchange contribution to the zero-field splitting tensor is substantial, since the largest component of **D** is not parallel to the Cu–Cu direction, as it would be for dominating dipolar contributions, but it is parallel to the highest **g** direction. This result is in agreement with those previously reported for other copper(II) dinuclear complexes in which the magnetic orbitals are roughly parallel to each other and coplanar.[5,23,24]

The g_{zz} directions correspond nicely to the axis of compression of the $CuCl_4$ tetrahedra, and also the increase of g_{zz} in the order *sb* < *as* < *p* agrees with the structural data, which show that *p* is the most severely distorted toward tetrahedral coordination. The $D_{z'z'}$ values show the same pattern, with a smooth increase on going from *sb* to *as* and *p*. The $D_{z'z'}$ values exceed the values expected for a dipolar interaction by $\sim 140 \times 10^{-4}$ cm^{-1}.

In a series of bis(μ-oxo)-bridged copper(II) complexes it has been suggested that $D_{z'z'}$ is negative and that the exchange contribution to it, $D_{z'z'}^{ex}$, is essentially determined by the interaction between the ground *xy* and the excited $x^2 - y^2$ orbital.[1,4-6] Since the ground orbital is similar also in these chlorocuprates, similar considerations should hold in the present case.

In the bis(μ-oxo)-bridged series we showed that $D_{z'z'}$ decreases on increasing the metal–metal distance and that for copper–copper distances as high as 3.3 Å the exchange contribution still outweighs the dipolar one. The data that we have now collected for the chloride-bridged complexes show that a similar relation holds, $D_{z'z'}$ decreasing when the Cu–Cu distance is increased. The rationale which we offered for the bis(μ-oxo)-bridged series was that, when the copper–ligand bond lengths are kept roughly constant, the Cu–L–Cu angle increases with increasing Cu–Cu distance, thus making less effective the overlap of the ligand orbital with the $x^2 - y^2$ orbital on one center and the *xy* orbital on the other metal center. As a consequence, the overlap density on the bridge atom decreases, and the coupling between the two metal ions decreases.[1]

Finally some considerations are in order about the observed temperature dependence of the EPR and electronic spectra. The increase of the energy of the electronic transitions on lowering the temperature seems to indicate that the coordination environment around the copper ions becomes close to the square-planar limit at low temperature. Recently it was suggested that a correlation can be established between the dihedral angle α and the energy of the near-IR transitions.[26-29] Using the relation of ref 26 and the structural parameters seen in the crystal structures,[8,9] we calculate the energy of the transition at 11 500 cm^{-1} for *sb*, 11 200 cm^{-1} for *as*, and 11 000 cm^{-1} for *p*, which are in agreement with the values observed at room temperature. On the other hand, if we use the energies of the transitions at 77 K to calculate the structural parameters at that temperature, we find $\alpha = 31°$ for *sb* and 33.5° for *as* and *p*, which indicates chromophores that are closer to the square-planar limit. The same conclusions can be reached by looking at the g_{zz} values of *sb*, which decrease on lowering the temperature. From this analysis it should be apparent that also *J* might be temperature dependent, thus making it even more difficult to draw precise structural–magnetic correlations with use of room-temperature structure data and one *J* value.

Registry No. $[(C_6H_5)_4P]_2Cu_2Cl_6$, 50860-38-3; $[(C_6H_5)_4Sb]_2Cu_2Cl_6$, 67597-60-8; $[(C_6H_5)_4As]_2Cu_2Cl_6$, 50807-65-3.

Supplementary Material Available: Listings of observed and calculated structure factors, thermal parameters for the non-hydrogen atoms, and positional parameters for the hydrogen atoms of $[(C_6H_5)_4Sb]_2Cu_2Cl_6$ (15 pages). Ordering information is given on any current masthead page.

(19) Roundhill, S. G. N.; Roundhill, D. M.; Bloomquist, D. R.; Landee, C.; Willett, R. D.; Dooley, D. M.; Gray, H. B. *Inorg. Chem.* **1979**, *18*, 831.
(20) Marsh, W. E.; Patel, K. C.; Hatfield, W. E.; Hodgson, D. J. *Inorg. Chem.* **1983**, *22*, 511.
(21) Hatfield, W. E. *Inorg. Chem.* **1983**, *22*, 833.
(22) Carlin, R. L.; Burriel, R.; Corneliesse, R. M.; Van Duyneveldt, A. J. *Inorg. Chem.* **1983**, *22*, 831.
(23) Kahn, O.; Galy, J.; Journaux, Y.; Jaud, J.; Morgenstern-Badarau, I. *J. Am. Chem. Soc.* **1982**, *104*, 2165.
(24) Bencini, A.; Benelli, C.; Dei, A.; Gatteschi, D., submitted for publication.
(25) Bencini, A.; Gatteschi, D. *Transition Met. Chem. (N.Y)* **1982**, *8*, 1–178.
(26) Battaglia, L. P.; Bonamartini-Corradi, A.; Marcotrigiano, G.; Menabue, L.; Pellacani, G. C. *Inorg. Chem.* **1979**, *18*, 148.
(27) Lamotte-Brassau, J. *Acta Crystallogr., Sect. A: Cryst. Phys., Diffr., Theor. Gen. Crystallogr.* **1974**, *A30*, 487.
(28) Willett, R. D.; Haugen, J. A.; Lebsack, J.; Morrey, J. *Inorg. Chem.* **1974**, *13*, 2510.
(29) Harlow, R. L.; Wells, W. J.; Watt, G. W.; Simonsen, S. H. *Inorg. Chem.* **1975**, *14*, 1768.